

MICROWAVE RADAR SENSING OF SEA WAVES: AN EFFECTIVE REFLECTION COEFFICIENT

V. Karaev^{*1} , M. Panfilova¹ , Yu. Titchenko¹ , E. Meshkov¹ , D. Kovaldov¹ , X. Li² , and Y. He² 

¹Institute of Applied Physics RAS, N. Novgorod, Russia

²School of Marine Sciences, Nanjing University of Information Science and Technology, Nanjing, China

* **Correspondence to:** V. Karaev, volody@ipfran.ru

Abstract: At the small incidence angles, the dominant backscattering mechanism for sea waves is the quasi-specular backscattering mechanism. The power of the reflected signal depends on the distribution function of the slopes of large-scale waves (in comparison with radar wavelength) and on the effective reflection coefficient, which is introduced instead of the Fresnel coefficient. In this paper, we discussed a new method for calculating the effective reflection coefficient from the wave scatterometer SWIM data. For the first time, measurements are performed by a radar at different azimuth angles at small incidence angles. This makes it possible to measure the effective reflection coefficient. An original algorithm was developed for data processing and determination of the total mean square slopes of large-scale sea waves and the azimuth dependence of the backscattering radar cross section at zero incidence angle. In the result of subsequent processing, the azimuth dependence of the effective reflection coefficient is retrieved. SWIM data were used to evaluate the developed algorithm. Processing of the test data set confirmed the efficiency of the algorithm. The azimuth anisotropy coefficients for the mean square slopes of large-scale waves and the effective reflection coefficient are calculated.

Keywords: microwaves, small incidence angles, Fresnel coefficient, effective reflection coefficient

Citation: Karaev, V., M. Panfilova, Yu. Titchenko, E. Meshkov, D. Kovaldov, X. Li, and Y. He (2023), Microwave Radar Sensing of Sea Waves: An Effective Reflection Coefficient, *Russian Journal of Earth Sciences*, 23, ES5001, EDN: TURMEQ, <https://doi.org/10.2205/2023es000850>

Introduction

To describe the backscattering of microwaves by the sea surface at small incidence angles the concept of a two-scale model (TSM) of the scattering surface was introduced. In accordance with it, the sea surface is represented as large-scale waves (in comparison with the radar wavelength), covered with small ripples. Thus, the concept of a boundary (so-called cut off) wave number is introduced, which divides the sea wave spectrum into large-scale waves, in comparison with radar wavelength, and small ripples.

Within the framework of the Kirchhoff's approximation, the mechanism of electromagnetic waves backscattering from the sea surface at small incidence angles is quasi-specular. Reflection occurs from facets of the wave profile oriented perpendicular to the incident radiation, and the backscattering radar cross section (RCS) depends on the mean square slopes (MSS) of large-scale wave. Small ripples located on the "large" wave lead to the appearance of diffuse (resonant) scattering, which reduces the power of the backscattering signal. To take this effect into account, the concept of the effective reflection coefficient (ERC) is introduced, which is used instead of the Fresnel coefficient in the formula for the RCS [Bass and Fuks, 1979; Valenzuela, 1978].

The complicated task of measuring the ERC has attracted attention for a long time. The first paper devoted to experiment was published in 1986 [Masuko et al., 1986]. The most detailed analysis of the dependence of the ERC on the wind speed was made in [Freilich and Vanhoff, 2003], where data from the precipitation radar (Ku-band) of the TRMM satellite were used. While moving, the precipitation radar scans by the incidence

RESEARCH ARTICLE

Received: 30 March 2023

Accepted: 6 July 2023

Published: 13 December 2023



Copyright: © 2023. The Authors. This article is an open access article distributed under the terms and conditions of the Creative Commons Attribution (CC BY) license (<https://creativecommons.org/licenses/by/4.0/>).

angle in a direction perpendicular to the flight track. As a result, the dependence of the RCS on the incidence angle is measured, and it can be used to retrieve the MSS along the scanning direction.

Since the MSS was calculated only along one azimuthal angle, the ERC was calculated using the assumption that large-scale waves are isotropic [Freilich and Vanhoff, 2003]. The use of this incorrect assumption is due to the lack of measurements of MSS at different azimuth angles. As a result, the ERC was calculated with an error.

The wave scatterometer SWIM, installed on the CFOSAT satellite, for the first time performs measurements at 24 azimuth angles, so the anisotropy of sea waves can be taken into account when calculating the ERC.

Discussion of the Retrieval Algorithm

At the small incidence angles, the backscattering radar cross section is given by the following formula [Bass and Fuks, 1979]:

$$\sigma_0(\theta_0, \varphi_{az}) = \frac{|R_{\text{eff}}(U_{10}, \varphi_{az}, \theta_0)|^2}{2 \cos^4 \theta_0 \sqrt{mss_{xx} mss_{yy} - mss_{xy}^2}} \exp \left[-\frac{\tan^2 \theta_0}{2(mss_{xx} mss_{yy} - mss_{xy}^2)} mss_{yy} \right], \quad (1)$$

where mss_{xx} and mss_{yy} – mean square slopes along X and Y axis respectively; mss_{xy} – the coefficient of cross-correlation of the slopes of large-scale waves mss_{xx} and mss_{yy} ; θ_0 – incidence angle; U_{10} – wind speed at the 10 m height; φ_{az} – wind direction; R_{eff} – effective reflection coefficient and $\text{ERC} = |R_{\text{eff}}|^2$. We assume that the sounding is carried out along the X axis and then the azimuth angle is equal to the angle between the wind direction and the sounding direction.

With an increase in wind speed, an increase in the MSS of large-scale waves and an increase in the spectral density of small ripples (variance of height) occur. As a result, the combined action of these factors leads to a decrease in the backscattering RCS at small incidence angles.

At a zero incidence angle, the formula (1) is simplified and takes the following form:

$$\sigma_0(0^\circ, \varphi_{az}) = \frac{|R_{\text{eff}}(U_{10}, \varphi_{az}, 0)|^2}{2 \sqrt{mss_{xx} mss_{yy} - mss_{xy}^2}}. \quad (2)$$

The effective reflection coefficient depends on the wind speed and the azimuth angle. The most important factor is the near-water wind speed, which has a significant effect on the amplitude of the ripple (the small-scale part of the sea wave spectrum). This can be seen from the dependence of resonant scattering at the middle incidence angles, when a change in wind speed leads to a change in the backscattering RCS by tens of decibels [Li et al., 2022b; Lin et al., 2012].

The next factor affecting the effective reflection coefficient is related to the azimuth dependence of the ripple spectral density. A change in wind direction will lead to a change in the spectral density along the sounding direction, which will change the effective reflection coefficient and, accordingly, the backscattering RCS.

To study the dependence of the effective reflection coefficient on the azimuth angle, the following approach is proposed.

The measurement of the backscattering RCS at small incidence angles at different azimuth angles is performed by the wave scatterometer SWIM installed on the Chinese-French CFOSAT satellite [Hauser et al., 2017, 2021].

For the first time radar performs measurements at 24 azimuth angles, so the anisotropy of sea waves can be taken into account when calculating the effective reflection coefficient. To calculate the effective reflection coefficient, the following method was used, which includes three stages.

At the first stage, using the well-known algorithm and the dependence of the RCS on the incidence angle is used to calculate the MSS of large-scale waves along the sensing direction (azimuth angle) [Chen et al., 2018; Chu et al., 2012; Freilich and Vanhoff, 2003; Hauser et al., 2008; Panfilova et al., 2020]. When retrieving the MSS, the RCS at zero incidence angle was also determined, which will be used further.

At the second stage the large-scale MSS calculated at the 12 or 24 azimuthal angles (after the first stage) are used for calculation of the azimuth dependence of large-scale slopes [Karaev et al., 2021; Li et al., 2022a]:

$$mss_{xx} = 0.5mss_{total} + 0.5\Delta mss \cdot \cos(2\varphi_0 - 2\varphi_{az}), \quad (3)$$

$$mss_{yy} = 0.5mss_{total} - 0.5\Delta mss \cdot \cos(2\varphi_0 - 2\varphi_{az}), \quad (4)$$

where $mss_{total} = mss_{xx} + mss_{yy}$, $\Delta mss = mss_{xx} - mss_{yy}$, and φ_0 direction of radar sensing.

Before processing, the preparation of SWIM data is performed so that the azimuth angle is measured from the expected (according to the numerical wind field model) wind direction. This data is made available to users. However, the real wind direction may not coincide with the estimates from the model, so the angle φ_0 is left in formulas (??) and (3) and it will be calculated. Thus, the direction of the wind may be clarified.

To estimate the coefficient of azimuth anisotropy of the MSS of large-scale waves, the following formula is used:

$$A_{az} = \frac{mss_{xx}}{mss_{yy}}. \quad (5)$$

At the third stage of processing, the model is used for calculation of mss_{xx} for azimuth angles of 0° and 90° relative to the direction of wave propagation. Here the real wind direction is used, which was determined in the second stage. Only in this case, the RCS at zero incidence angle (the result of the first stage) and the MSS are related by a simple analytical formula.

As a result, the ERC is calculated for two azimuth angles: 0° and 90° , for example.

$$|R_{\text{eff}}(0^\circ, 90^\circ)|^2 = \frac{\sigma_0(0^\circ, 90^\circ)}{2\sqrt{mss_{xx}mss_{yy}}} = \text{ERC}, \quad (6)$$

$$|R_{\text{eff}}(0^\circ, 0^\circ)|^2 = \frac{\sigma_0(0^\circ, 0^\circ)}{2\sqrt{mss_{xx}mss_{yy}}} = \text{ERC}. \quad (7)$$

In this case, the coefficient of azimuth asymmetry of the mss of large-scale waves K_{az} will be equal to

$$K_{az} = \frac{|R_{\text{eff}}(0^\circ, 0^\circ)|}{|R_{\text{eff}}(0^\circ, 90^\circ)|}.$$

The value of the cross-correlation coefficient is much less than the MSS of large-scale waves; therefore, it can be neglected in formula (2) and this formula can be tried to use for all azimuth angles. As a result, an estimate of the azimuth dependence of the effective reflection coefficient will be obtained.

Example of Data Processing

Let us illustrate the operation of the proposed processing method on SWIM data. The input data are the backscattering RCS measured at different incidence angles and different azimuth angles. Data are analyzed that refer to a section of the sea surface measuring 70×180 km (24 azimuth angles) or 70×90 km (12 azimuth angles).

At the first stage, the dependence of the backscattering RCS on the incidence angle is analyzed and the MSS of large-scale wave are calculated for 24 (or 12) azimuth angles. The result is shown in Figure 1 by stars. In addition, the backscattering RCS for a zero incidence angle is retrieved.

The retrieved MSS are the input parameters for the second processing stage. Regression is performed and the coefficients of the model are found (see formula (3)). For this example, $mss_{total} = 0.0319$; $\Delta mss = 0.0016$ and $\varphi_0 = 5^\circ$. On Figure 1 this dependence is shown by a solid curve.

The azimuth asymmetry coefficient for slopes is $A_{az} = 1.11$.

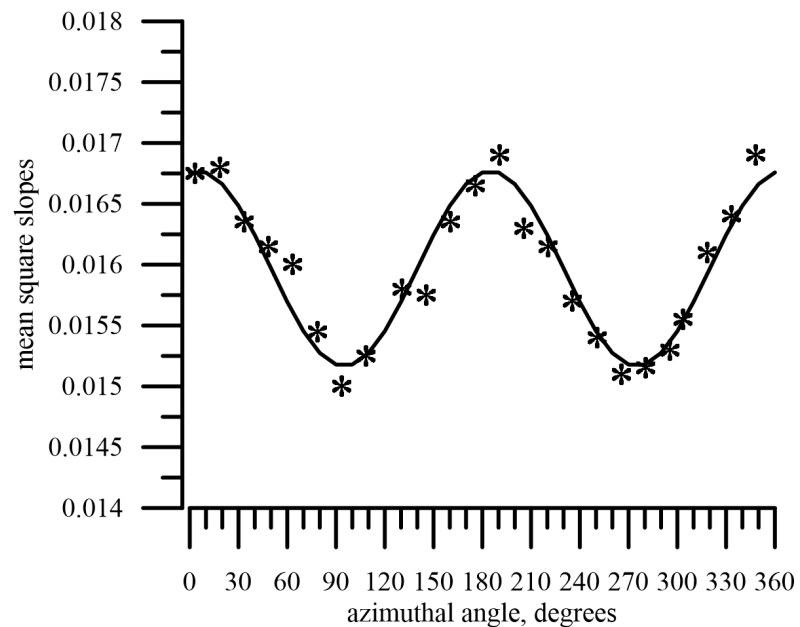


Figure 1. Azimuth dependence of the mss_{xx} of large-scale waves: asterisks – retrieved values, curve – model.

Simultaneously with the MSS of the large-scale waves, the RCS for a zero incidence angle were retrieved, and the result is shown in Figure 2. The asterisks show the RCS retrieved in the course of processing. The curve shows the result of the regression.

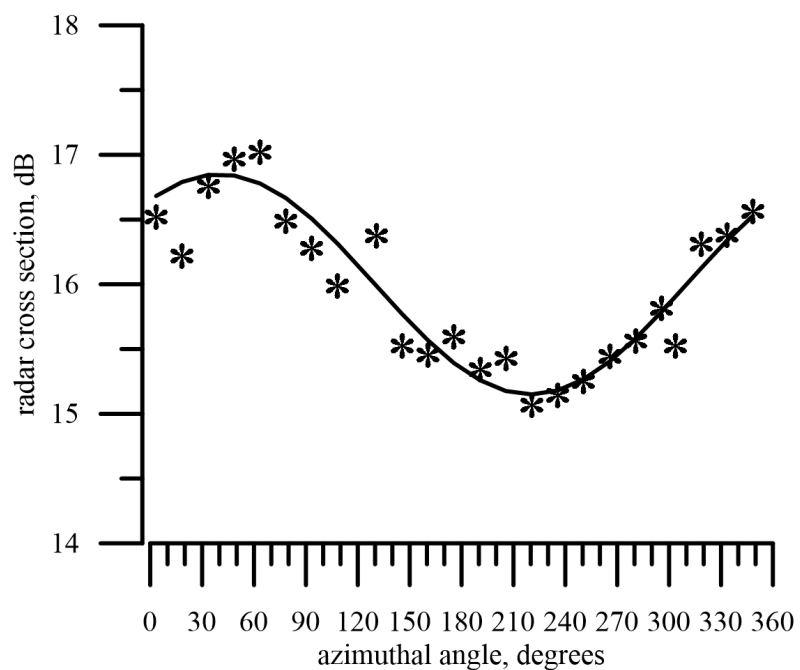


Figure 2. Azimuth dependence of the RCS at zero incidence angle: asterisks – retrieved values, curve – result of the regression.

The observed fluctuations of the initial data in Figures 1 and 2 can be caused by different reasons, in particular, due to insufficient averaging or wave variability in a 70×180 km area. It is impossible to make the right choice without additional analysis; therefore, when performing calculations at the third stage, we will consider both options: calculated data and a model data.

In the first case, we use the data that were obtained during processing and are shown in the figures with asterisks. In the second variant, we use the model data (result of the regression analysis) that were obtained during processing (curves in the figures).

To calculate the effective reflection coefficient, formula (6) is used and Figure 3 shows the results of the calculations. Here the input parameters from Figure 1 and Figure 2 were used.

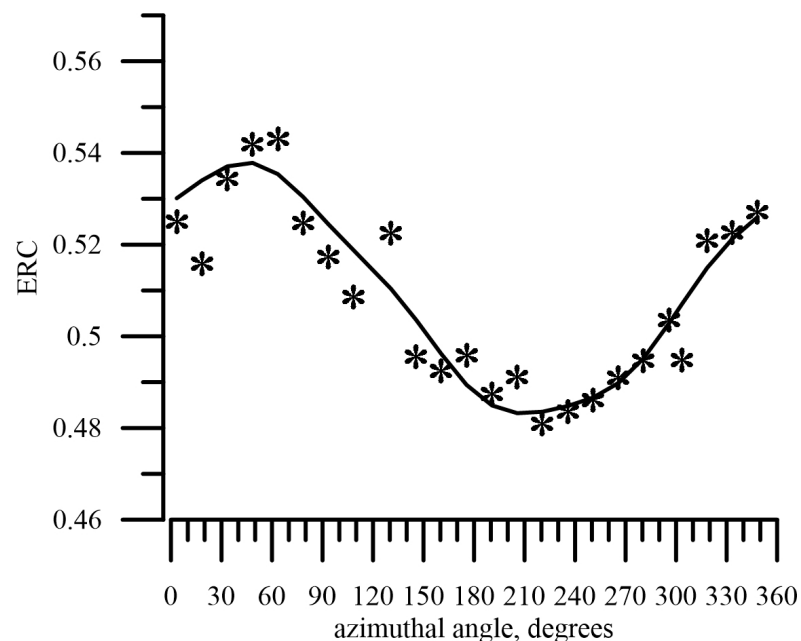


Figure 3. Azimuth dependence of the ERC: asterisks – according to experimental data and curve – according to formula (6) with input parameters from Figure 1 and Figure 2.

It can be seen from the figure that the dependences obtained by both methods are similar and, therefore, can be used to study the effective reflection coefficient.

In this case, the asymmetry coefficient is equal to $K_{az} = 1.11$.

The next step is the evaluation of the retrieval precision of the ERC (5). To do this, it is necessary to have data from independent contact measurements, but such measurements are unknown to us. To obtain a rough estimate, we use the following approach.

Let us represent the azimuthal dependence of the MSS of large-scale waves, taking into account the Δmss error, in the following form

$$mss_{xx}mss_{yy} = mss_{xx}mss_{yy} + \Delta mss.$$

The results of numerical simulation showed that the relative error ε_{mss} according to numerical simulation does not exceed 15–20%. The calculations were performed under the assumption of a known value of the ERC.

Measurements of the RCS are also performed with an error of no more than $\Delta\sigma$:

$$\sigma_0 = \sigma_0 + \Delta\sigma.$$

It is known from the requirements for orbital radars that the absolute error in measuring the RCS does not exceed 2 dB.

Table 1. Relative measurement error of the RCS

RCS, dB	Relative error, %	Intensity of sea waves
8	25	high
14	6	medium
20	2	low

Formulas (6) and (7) are used to calculate ERC, so the relative error in determining ERC does not exceed the following value

$$\varepsilon_{ERC} < \varepsilon_{RCS} + 0.5\varepsilon_{MSS},$$

where ε_{RCS} is the relative measurement error of the RCS. Table 1 shows the relative errors for typical RCS, assuming that the absolute error does not exceed 2 dB for all values of RCS.

Thus, the relative error in determining the effective reflection coefficient is less than 10–12% for low intensity of sea waves and less 33–35% for high intensity of sea waves.

Conclusions

The original method for calculating the effective reflection coefficient from the wave scatterometer SWIM data is developed. The algorithm consists of three stages. Firstly, in data processing the total MSS of large-scale wave slopes is calculated, the azimuth anisotropy is determined, and the wind direction is refined. At the second stage the azimuth dependence of the backscattering RCS at a zero incidence angle is also determined. And at the third stage in the course of subsequent processing, the azimuth dependence of the effective reflection coefficient is retrieved.

SWIM data can be used to evaluate the performance of the developed algorithm. Processing of the test data set confirmed the efficiency of the algorithm. The azimuth anisotropy coefficients for the MSS of large-scale waves and the effective reflection coefficient are calculated.

It is planned to process the SWIM data and calculate the dependence of the effective reflection coefficient on the wind speed.

Acknowledgement. The study was carried out at the expense of a grant from the Russian Science Foundation (project No. 20-77-10089).

References

- Bass, F. G., and I. M. Fuks (1979), *Wave Scattering from Statistically Rough Surfaces*, 528 pp., Elsevier, <https://doi.org/10.1016/c2013-0-05724-6>.
- Chen, P., G. Zheng, D. Hauser, and F. Xu (2018), Quasi-Gaussian probability density function of sea wave slopes from near nadir Ku-band radar observations, *Remote Sensing of Environment*, 217, 86–100, <https://doi.org/10.1016/j.rse.2018.07.027>.
- Chu, X., Y. He, and G. Chen (2012), Asymmetry and Anisotropy of Microwave Backscatter at Low Incidence Angles, *IEEE Transactions on Geoscience and Remote Sensing*, 50(10), 4014–4024, <https://doi.org/10.1109/tgrs.2012.2189010>.
- Freilich, M. H., and B. A. Vanhoff (2003), The Relationship between Winds, Surface Roughness, and Radar Backscatter at Low Incidence Angles from TRMM Precipitation Radar Measurements, *Journal of Atmospheric and Oceanic Technology*, 20(4), 549–562, [https://doi.org/10.1175/1520-0426\(2003\)20<549:trbwsr>2.0.co;2](https://doi.org/10.1175/1520-0426(2003)20<549:trbwsr>2.0.co;2).
- Hauser, D., G. Caudal, S. Guimbard, and A. A. Mouche (2008), A study of the slope probability density function of the ocean waves from radar observations, *Journal of Geophysical Research*, 113(C2), <https://doi.org/10.1029/2007jc004264>.
- Hauser, D., C. Tison, T. Amiot, L. Delaye, N. Corcoral, and P. Castillan (2017), SWIM: The First Spaceborne Wave Scatterometer, *IEEE Transactions on Geoscience and Remote Sensing*, 55(5), 3000–3014, <https://doi.org/10.1109/tgrs.2017.2658672>.
- Hauser, D., C. Tourain, L. Hermozo, D. Alraddawi, L. Aouf, B. Chapron, A. Dalphinnet, L. Delaye, M. Dalila, E. Dormy, F. Gouillon, V. Gressani, A. Grouazel, G. Guitton, R. Husson, A. Mironov, A. Mouche, A. Ollivier, L. Oruba, F. Piras, R. R. Suquet, P. Schippers, C. Tison, and N. Tran (2021), New Observations From the SWIM Radar On-Board CFOSAT: Instrument Validation and Ocean Wave Measurement Assessment, *IEEE Transactions on Geoscience and Remote Sensing*, 59(1), 5–26, <https://doi.org/10.1109/tgrs.2020.2994372>.

- Karaev, V. Y., M. A. Panfilova, M. S. Ryabkova, Y. A. Titchenko, E. M. Meshkov, and X. Li (2021), Retrieval of the two-dimensional slope field by the SWIM spectrometer of the CFOSAT satellite: discussion of the algorithm, *Russian Journal of Earth Sciences*, 21(6), 1–9, <https://doi.org/10.2205/2021es000784>.
- Li, X., V. Karaev, M. Panfilova, B. Liu, Z. Wang, Y. Xu, J. Liu, and Y. He (2022a), Measurements of Total Sea Surface Mean Square Slope Field Based on SWIM Data, *IEEE Transactions on Geoscience and Remote Sensing*, 60, 1–9, <https://doi.org/10.1109/tgrs.2022.3174392>.
- Li, X., W. Lin, B. Liu, Z. Wang, B. Zhang, and Y. He (2022b), Sea Surface Wind Retrieval Using the Combined Scatterometer and Altimeter Backscatter Measurements of the HY-2B Satellite, *IEEE Transactions on Geoscience and Remote Sensing*, 60, 1–12, <https://doi.org/10.1109/tgrs.2021.3065663>.
- Lin, C.-C., M. Betto, M. B. Rivas, A. Stoffelen, and J. de Kloe (2012), EPS-SG Windscatterometer Concept Tradeoffs and Wind Retrieval Performance Assessment, *IEEE Transactions on Geoscience and Remote Sensing*, 50(7), 2458–2472, <https://doi.org/10.1109/tgrs.2011.2180393>.
- Masuko, H., K. Okamoto, M. Shimada, and S. Niwa (1986), Measurement of microwave backscattering signatures of the ocean surface using X-band and Ka-band airborne scatterometers, *Journal of Geophysical Research*, 91(C11), 13,065, <https://doi.org/10.1029/jc091ic11p13065>.
- Panfilova, M., V. Karaev, L. Mitnik, Y. Titchenko, M. Ryabkova, and E. Meshkov (2020), Advanced View at the Ocean Surface, *Journal of Geophysical Research: Oceans*, 125(11), <https://doi.org/10.1029/2020jc016531>.
- Valenzuela, G. R. (1978), Theories for the interaction of electromagnetic and oceanic waves – A review, *Boundary-Layer Meteorology*, 13(1-4), 61–85, <https://doi.org/10.1007/bf00913863>.